

# DYNAMIC FLUID STRUCTURE INTERACTION OF A FOIL

**C. Lothodé**, K-Epsilon, France, corentin@k-epsilon.com

**M. Durand**, K-Epsilon, France, mathieu@k-epsilon.com

**Y. Roux**, K-Epsilon, France, yann@k-epsilon.com

**A. Leroyer**, École Centrale de Nantes, France, alban.leroyer@ec-nantes.fr

**M. Visonneau**, École Centrale de Nantes, France, michel.visonneau@ec-nantes.fr

**L. Dorez**, Groupama Sailing Team, France, loic@groupamasailingteam.com

In this paper, a dynamic computation of the Groupama 3 foil is performed. Foils are thin profiles, placed under the hull of a ship, allowing it to provide a lifting force. This study is placed in the context of the 2013 America's Cup, which will see the appearance of a new kind of high performance multihull.

At high speeds, the foils are subject to intense hydrodynamic forces and to movement due to the sea state. The deformations are then sizable and there is a risk of ventilation, cavitation or vibration which could lead to a large modification of the hydrodynamic forces or to the destruction of the foil.

The foil being light compared to the added mass effect, the interaction is a strongly coupled problem. In this paper, the problem is solved using a segregated approach. The main problems resulting of such a method are the numerical stability and remeshing. These problems are detailed and some results presented.

As a first test case, the simulation of a vortex excited elastic plate proposed by Hubner is presented. This case is very demanding in terms of coupling stability and mesh deformation.

Then, the foil of Groupama 3 is modelled in a simplified form without hull and free surface, and then in a more realistic conditions with free surface and waves.

## NOMENCLATURE

$\mu$	Kinematic viscosity	( $\text{N.s.m}^{-2}$ )
$\rho$	Density of water	( $\text{kg.m}^{-3}$ )
$P$	Pressure	( $\text{N.m}^{-2}$ )
$F$	Force	(N)
$M$	Moment	(N.m)
$x, y, z$	Positions	(m)
$t$	Time	(s)

## 1 NUMERICAL METHOD

The strategy used to solve the fluid structure interaction problem is a partitioned coupling between a fluid solver and a structural solver. The two solvers are described in the following as well as the coupling algorithm.

### 1.1 FLUID: ISIS-CFD

The solver ISIS-CFD included in FINE/Marine<sup>TM</sup> is developed by the DSPM team of LHEEA laboratory. It solves the Reynolds-Averaged Navier-Stokes Equations in a strongly conservative way. It is based on the finite volume method and can work on structured or unstructured meshes with arbitrary polyhedrons [1].

The velocity field is obtained from the momentum conservation equations and the pressure field is extracted from the incompressibility constraint. The pressure-velocity coupling is achieved through a SIMPLE-like algorithm. All the vari-

ables are stored in a cell-centered manner. Volume and surface integrals are evaluated with second order discretization. The time integration is an implicit scheme of order two. At each time step, an internal loop is performed (called a non-linear iteration) associated with a Picard linearization in order to solve the non-linearities of the Navier-Stokes equations.

The equations are formulated according to the Arbitrary Lagrangian Eulerian paradigm and therefore can easily take into account mesh deformations. Several turbulence models are implemented in ISIS-CFD. In this study, we used the SST- $k - \omega$  model [2].

### 1.2 STRUCTURE: ARA

The solver ARA was developed by the company K-Epsilon during the project VOILEnav [3]. The code was initially aimed at simulating the dynamic behaviour of sailboat rigs : sails, mast and cables.

A non-linear finite element method with a large deformation formulation is implemented. At each time step, an equilibrium between external and internal forces is sought between all the elements and forces acting on them. The elements receive as an input the position, the speed and the acceleration of each of its nodes. It can contain internal variables in the case of elastic deformation, and the element computes the derivatives of forces according to those variables. These derivatives are assembled into a mass matrix  $[M] = \frac{\partial F}{\partial \bar{x}}$ , damping matrix  $[D] = \frac{\partial F}{\partial \dot{\bar{x}}}$  and stiffness matrix  $[K] = \frac{\partial F}{\partial \bar{x}}$ . Elements can be composed of different kind of finite elements

(cable, beam, shell, membrane). It is also possible to use elements with a penalization method such as contact or sliding elements. In the coupling algorithm, the fluid-structure interface itself is considered as an element.

The time scheme used is the Newmark-Bossak scheme (second order accurate). This scheme has been chosen for its compromise between the necessary filtering of the high frequencies while maintaining the accuracy of the low frequencies. The scheme is conservative hence avoids numerical energy creation in case of large non-linearities.

### 1.3 ELEMENT USED

While numerous element types have been implemented in the structural code, in the present study, only beam elements are used. These elements are Timoshenko elements, with the hypothesis of small deformations. We therefore have a constant stiffness matrix in the local frame. Each beam element is defined thanks to two points (for position) and two quaternions (for the tangent directions). More details on the non-linear algorithm used can be found in [4].

### 1.4 COUPLING

The fluid-structure coupling leads to four problems:

- the continuity of constraints at the interface ;
- the deformation of the interface ;
- the deformation of the fluid mesh ;
- the coupling algorithm.

#### 1.4.1 Continuity of constraints

The perfect continuity of constraints cannot be assured because of the difference between the fluid discretisation and the structural discretisation. Thus, a consistent method is used (see [4]). The method corresponds to an integration of the forces on the fluid faces :

$$\mathbf{F}_M = \int_{\Gamma} (p \mathbf{n} + \boldsymbol{\tau} \cdot \mathbf{n}) d\Gamma$$

and then a projection of those efforts on the degree of freedom of the closest beam element.

#### 1.4.2 Interface deformation

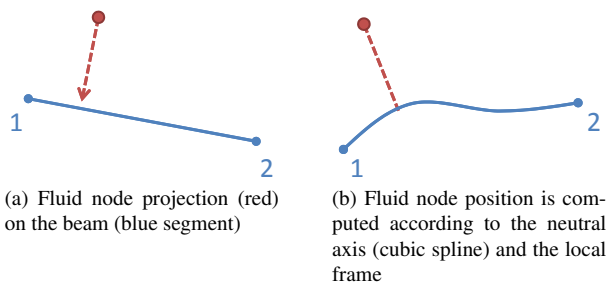


Figure 1: Fluid structure interface deformation.

The fluid structure interface is entirely defined by the fluid faces. Each fluid node is projected onto the nearest beam elements in order to get a parameterized position of the projected point as well as a vector linked to the local frame of the beam. When the beam is deformed, the 3D deformation of the neutral axis is computed with the variation of the local frame from one end to the other end of the beam. The local frame evolves smoothly according to a cubic spline law. Therefore, the new fluid node position is computed from the new position of the neutral axis and its local frame (see Figure 1).

### 1.4.3 MESH DEFORMATION

Following the interface deformation, the whole mesh of the fluid domain needs to be deformed. This deformation occurs at each coupling iteration. The number of call to this procedure being non-negligible, the mesh deformation needs to be fast. To do this, a new method was developed that propagates the deformation state to the fluid mesh. The algorithm is described more thoroughly in [4]. The rigid displacement (translation and rotation) of each face of the interface is computed. This displacement is propagated to its neighbours and so on iteratively until the boundaries of the mesh are reached.

### 1.4.4 QUASI-MONOLITHIC ALGORITHM

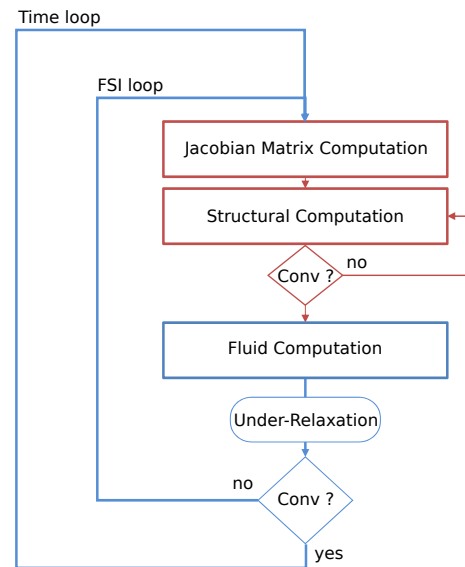


Figure 2: Dynamic coupling algorithm. In blue, the fluid solving scheme. In red, the added structural iteration with the Jacobian computation.

The global solution algorithm is based on a quasi-monolithic approach. This approach is an implicit coupling adapted to a partitioned solver while conserving the property of convergence and stability of the monolithic approach. To obtain such a result, the structural computation is performed at each non-linear iteration of the fluid (inner loop). The fluid algorithm is not modified. The non-linear iterations include a fluid subiteration and a structural convergence. The

non-linear iterations are performed until convergence, therefore fluid-structure convergence is reached at each time step. Furthermore, an "interface" element is added to the structural solver. This element is computed from the Jacobian matrix of the interface. In the case of an exact Jacobian matrix, the algorithm is the same as a monolithic algorithm. With the same idea as the quasi-Newton method where a simplified Hessian matrix is used, here a simplified Jacobian is computed.

The Jacobian matrix is not necessary, even for strongly coupled problems. Nonetheless, its use permits the elimination of under-relaxation, implying a significant reduction in the number of coupling iterations required.

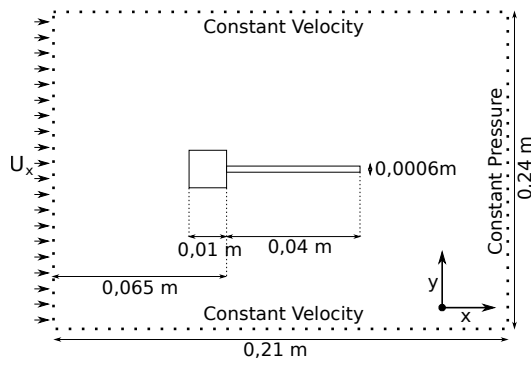
With the present method, the ratio between the time of fluid structure interaction and fluid only computations is in between 1 and 2.

## 2 TEST CASES

### 2.1 HUBNER TEST

To start, an academic test was studied [5]. This case is itself a modification of [6] by changing certain boundary condition and characteristics of the structure. With the case of Hubner, the structure is more bendable and the deformations are larger. The case is therefore harder to study.

The parameters of Hubner were studied by Valds et Vázquez [7] and also by Guillaume De Nayer in 2008 [8]. The later modified the dimensions of the domain which he found to be too small. Those dimensions are used here (c.f. Figure 3a and TABLE 3b).



(a) Diagram of the simulation domain

Fluid data			
Fluid density	$\rho_f$	1,18	$kg.m^{-3}$
Dynamic viscosity	$\mu_f$	$1,82 \times 10^{-5}$	$Pa.s$
Inlet velocity	$U_x$	0,315	$m.s^{-1}$
Structural data			
Square size	$a$	0,01	$m$
Length of the tip	$L$	0,04	$m$
Tip thickness	$d$	0,0006	$m$
Young modulus	$E$	0,2	$MPa$
Tip density	$\rho_s$	2000	$kg.m^{-3}$
Poisson coefficient	$\nu$	0,35	

(b) Properties of the fluid and the structure

Figure 3: Description of the benchmark

According to the data, the Reynolds number is 200. The assumption of a laminar flow was used. The physical time of the computation is approximately 25 s and the time step is  $\Delta t = 0.001s$ . The fluid mesh was generated by HEXPRESS<sup>TM</sup>, the mesher of the software FINE/Marine<sup>TM</sup>. It has 111452 cells and 132782 vertices. The structural beam is made out of 100 beam elements.

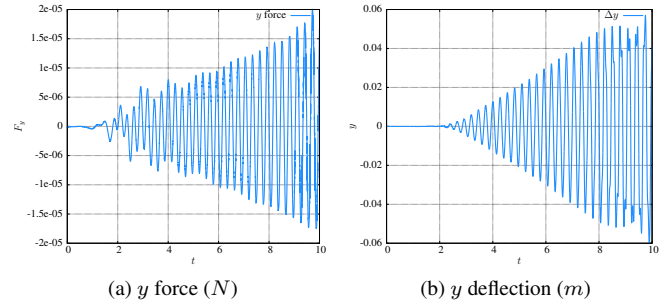
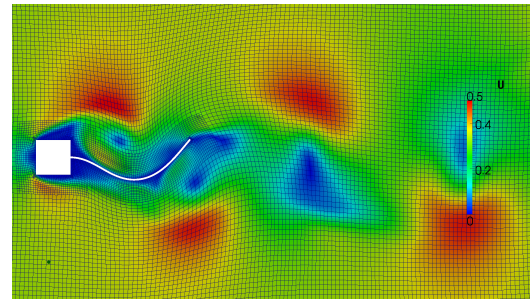


Figure 4: Evolution of forces and deformation

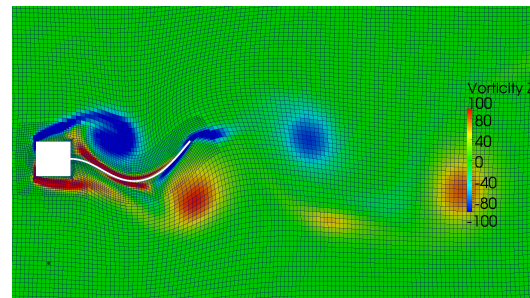
The results obtained by Hubner show an amplitude of 6cm and correspond to the results obtained by the method presented here. Furthermore, the frequency ( $3.15 \pm 0.05Hz$ ) is also in the range obtained by Hubner and De Nayer (3.22Hz for De Nayer, 3.10Hz for Hubner).

Figure 5 shows the results of the mesh deformation. The cell quality and orientation is preserved even with relatively large deformation.

The tip oscillates in phase with the creation of vortices by the square block. We can see these vortices advected in the flow in Figure 5b.



(a)  $\|u\|$



(b)  $\omega_z$

Figure 5: Visualization of the mesh deformation and creation of vortices in established flow

## 2.2 DAGGERBOARD

A daggerboard is providing side force to counter the force produced by the sail. Recently on multihulls, it is also used to provide lift force, either as a lift assist foil<sup>1</sup> or a fully lifting foil<sup>2</sup>. Most of the time, the influence of the daggerboards can be modified by modifying their orientation and position.

The study is done on the foil of Groupama 3, trimaran of 105 feet (32 m) and 18 tons. The boat broke the Jules Verne record (fastest circumnavigation around the world) in 2010. This boat represents a breakthrough in the concept of oceanic racing yachts by being lighter and by including hydrofoils.

The foil used by Groupama 3 is a C foil, which is the shape you can see by looking at it by the front side. It also has a winglet to reduce the induced drag.



Figure 6: Groupama 3

### 2.2.1 QUASI-STATIC CASE OF A FOIL ALONE

In this case, a simplified version of the foil is used. The foil is simply an extrusion of a NACA 4512 profile, with a curvature radius of  $3m$ , without the winglet. Furthermore, we do not take into account the free surface.

The structural mesh is given by 14 beam elements, with the node at the highest elevation blockfixed in both position and rotation.

The first step is a quasi-static computation to predict the equilibrium position of the foil. Fluid iterations are performed alone until convergence, then a structural convergence is performed. The mesh is updated and a new fluid convergence with the new deformed mesh is performed. The quasi-static loop is done until convergence of the geometry. This convergence is assured only if the problem is stable.

The results obtained show a deflection of  $0.595m$  and a change in forces of  $1.882 \times 10^4$  N (for an initial  $F_z$  force of  $7.434 \times 10^4$  N). Those results were obtained with an inlet velocity of  $15m \cdot s^{-1}$ .

The gain in lift is big (+25%) whereas the drag is only augmented by a small factor (+3%). By adjusting correctly the neutral axis and the center of effort, this behaviour can be optimized. At this speed, for a deformed foil, the lift represents 50% of the weight of the boat.

<sup>1</sup>to reduce the drag by reducing the immersed volume of the hull, which is the case of most sailing multihulls

<sup>2</sup>hull out of the water, like the Hydroptre

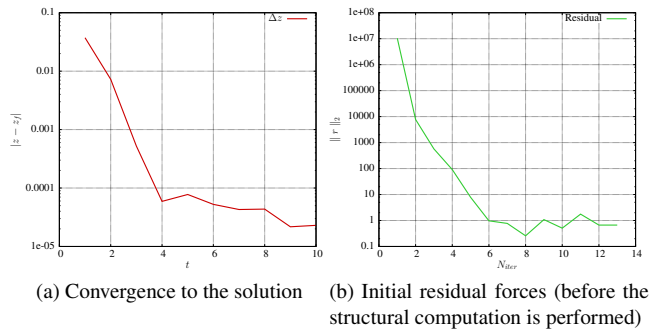


Figure 7: Convergence

The Figure 7 shows the quasi-static convergence. We notice that the deflection obtained is converged. The initial residual of the coupling (before computation of the structure) is decreasing by an order of magnitude at each coupling iteration. The solution is converged with only 6 quasi-static iterations.

## 2.3 VIBRATION STUDY : FLUTTER

Starting from a quasi-static computation, it is possible to study vibratory behavior such as flutter. Flutter is a self-feeding and potentially destructive vibration. If the energy input by the hydrodynamic excitation in a cycle is larger than that dissipated by the damping in the system, the amplitude of vibration will increase, resulting in self-exciting oscillation. The prediction of such phenomenon is done through dynamic fluid-structure interaction computations.

First, a quasi-static convergence is done on a configuration where the neutral axis is  $35cm$  away from the leading edge (almost in the middle of the chord), with an added momentum at the tip of the foil and with an inlet velocity of  $10m \cdot s^{-1}$ .

Then, the structure is released (no added momentum at the tip) and a dynamic computation is performed. The timestep used during the computation is  $10^{-4}s$ . It is to be noted that only 13 non-linear iterations are required to reach convergence at each time step when 10 are required with the fluid only (no structure).

In Figure 8a and 8c, it is possible to notice that the frequencies involved are not the same: about 200 Hz for the forces whereas the displacement shows a frequency of approximately 10 Hz. It is possible to notice that on this case, the vibration is not self-feeding and a damping occurs on the displacement.

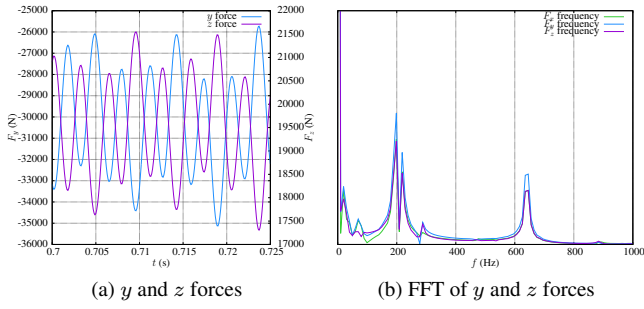
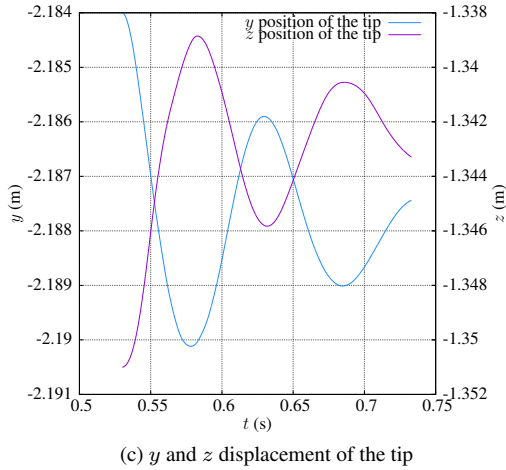
(a)  $y$  and  $z$  forces(b) FFT of  $y$  and  $z$  forces(c)  $y$  and  $z$  displacement of the tip

Figure 8: Forces in time and frequency domain, and the displacement of the tip with respect to time

### 2.3.1 FOIL WITH HULL AND WAVES

In this section, the real geometry of the foil (including the wingle) is used and the hull is added. Unsteady fluid structure interaction computations were performed with the foil fixed at the interface of the hull. A free surface is imposed at  $z = 0$  as an initial condition. The hull is fixed and all of the nodes of the beam inside the hull are fixed in both translation and rotation.

At  $t = 0s$ , the speed of the boat is  $0m \cdot s^{-1}$ . The imposed motion is done according to a  $\frac{1}{4}$  sinusoidal law until  $15m \cdot s^{-1}$ . The waves are starting at  $t = 0s$ ,  $45m$  in front of the foil and reach the foil at  $t = 6s$ . The waves are Stokes first order potential waves with  $1m$  wave height and a period of  $3s$ .

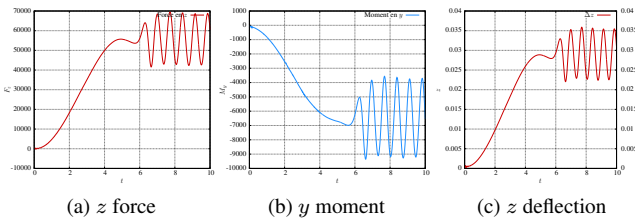
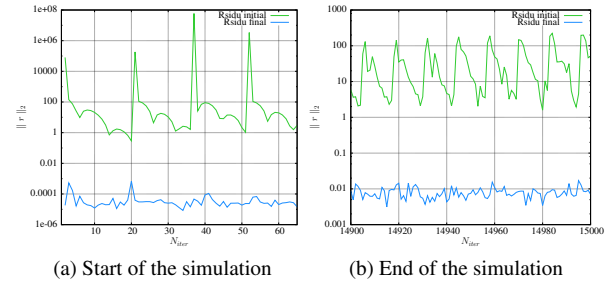
(a)  $z$  force(b)  $y$  moment(c)  $z$  deflection

Figure 9: Forces and momentum acting on the foil with respect to time

Figure 9a and Figure 9b show the variation of the lift forces and torsion moment in the foil local frame. The variation of



(a) Start of the simulation

(b) End of the simulation

Figure 10: Initial residual on the structure

lift is  $56 \pm 12kN$ .

The foil is very stiff and therefore does not bend very much. Nonetheless, the amplitude observed in waves is not negligible because it induces a vertical velocity that changes the incident flow, and thus the lift and drag.

The Figure 10 permits us to conclude on the convergence of the coupling. It can be seen that the initial residual decreases quickly during the non-linear iterations until convergence. Furthermore, using the Jacobian matrix of the interface allows a convergence in 20 subiterations where a classic implicit coupling with under-relaxation would require about a hundred subiterations. A computation without fluid structure interaction needs about 10 iterations to reach convergence.

## 3 CONCLUSION

The results of a partitioned coupling between a viscous, incompressible fluid solver and a structural finite element analysis software are presented for strongly coupled problems. The Hubner case permitted the validation of the fluid-beam interaction. The quasi-static and dynamic results for the daggerboard of a high performance multihull were then presented.

Furthermore, the design scope of this yacht was to do oceanic races and therefore it was designed to be both very reliable and safe. Thus, the foils used are smaller compared to what can be used for smaller, 60 foot (18 m) ORMA multihulls of the same generation. To use bigger foils on maxi trimaran, it will be necessary to predict the dynamic stability of the boat and also to dimension their structure.

Vibratory phenomena such as flutter, which can lead to failure of the foil were investigated and the ability of the code to simulate such behavior proven.

The boundary conditions for the structure play an important role in the determination of the structural deflections, hence it would be of interest to investigate a freely moving foil inside the hull with pinned connections at the lower and upper hull surfaces which corresponds more closely to what is happening in reality.

## ACKNOWLEDGEMENTS

We would like to thank PACAGrid and INRIA for providing the computational power required to undertake this study.

## REFERENCES

- [1] J. Wackers, B. Koren, H. Raven, A. van der Ploeg, A. Starke, G. Deng, P. Queutey, M. Visonneau, T. Hino, and K. Ohashi, "Free-surface viscous flow solution methods for ship hydrodynamics," *Archives of Computational Methods in Engineering*, vol. 18, no. 1, pp. 1–41, 2011.
- [2] F. Menter, M. Kuntz, and R. Langtry, "Ten years of industrial experience with the sst turbulence model," *Turbulence, heat and mass transfer*, vol. 4, pp. 625–632, 2003.
- [3] B. Augier, P. Bot, F. Hauville, and M. Durand, "Experimental validation of unsteady models for fluid structure interaction: Application to yacht sails and rigs," *Journal of Wind Engineering and Industrial Aerodynamics*, vol. 101, pp. 53–66, 2012.
- [4] M. Durand, *Interaction fluide-structure souple et legere, applications aux voiliers*. PhD thesis, Ecole Centrale Nantes, 2012.
- [5] B. Hübner, E. Walhorn, and D. Dinkler, "A monolithic approach to fluid–structure interaction using space–time finite elements," *Computer methods in applied mechanics and engineering*, vol. 193, no. 23, pp. 2087–2104, 2004.
- [6] E. Ramm and W. Wall, "Fluid-structure interaction based upon a stabilized (ale) finite element method," 1998.
- [7] J. Valds, J. Miquel, and E. Oate, "Nonlinear finite element analysis of orthotropic and prestressed membrane structures," *Finite Elements in Analysis and Design*, vol. 45, no. 67, pp. 395 – 405, 2009.
- [8] G. De Nayer, *Interaction Fluide-Structure pour les corps lancés*. PhD thesis, cole Centrale de Nantes, 2008.

## 4 AUTHORS BIOGRAPHY

**C. Lothode** holds the current position of R&D engineer at K-Epsilon. He is responsible for FSI computations and development. His previous experience includes a M.Sc. in Applied Mathematics.

**M. Durand** holds the current position of R&D director at K-Epsilon. He is responsible for FSI developments and sails simulations. His previous experience includes a PhD in fluid dynamic in 2012, and is also a world ranker match racing skipper (#40 in world ranking in 2011).

**Y. Roux** holds the current position of CEO of K-Epsilon. His previous experience includes a PhD in fluid mechanics. He did multiple study on victorious yacht such as Groupama 3 and 4.

**A. Leroyer** holds the current position of Associate Professor at the LHEEA laboratory of Ecole Centrale Nantes. His research topics revolve around the numerical modelling of the incompressible isothermal flows around complex geometries and are more specifically focused on the methodologies to integrate new physical phenomena inside a Navier-Stokes solver, as the fluid-structure interaction and the numerical modelling of cavitation. He is part of the developer team of

ISIS-CFD. His previous experience includes a PhD in fluid dynamics in 2004.

**M. Visonneau** holds the current position of Research Scientist of the CNRS at the LHEEA laboratory of Ecole Centrale Nantes. His main research topics are Computational Fluid Dynamics (CFD), Ship Hydrodynamics and Turbulence Modeling for high Re flows. In 1991, he got the 2nd Cray Prize for CFD and has been awarded 30th Georg Weinblum Memorial Lecturer (2007-2008) in 2007. His previous experience includes the head of the CFD department of the Fluid Mechanics Laboratory (ECN) from 1995 to 2012.

**L. Dorez** holds the current position of head of the Groupama Sailing Team.